

## Synthesis of Aniline – Pyrrole Copolymer Nanostructures by the Pulsed Galvanostatic Polymerization

Hassan Karami<sup>1,\*</sup>, Samaneh Jafari<sup>2</sup>, Fariba Goli<sup>2</sup>

<sup>1</sup> Department of Chemistry, Payame Noor University, 19395-4697, Tehran, I.R. of Iran

<sup>2</sup> Nano Research Laboratory, Department of Chemistry, Payame Noor University, Abhar, Iran

\*E-mail: [karami\\_h@yahoo.com](mailto:karami_h@yahoo.com)

Received: 18 November 2015 / Accepted: 6 February 2016 / Published: 1 March 2016

---

In this work, aniline- pyrrole copolymer (APC) nanoparticles are synthesized by the pulsed galvanostatic polymerization method. Two cylindrical platinum grid electrodes with diameters of 1 and 3cm are used as coaxial in the electrochemical cell containing aniline, pyrrole and HCl solution. Aniline and pyrrole are directly oxidized to aniline and pyrrole cation radicals as polymeric precursors on the surface of platinum anode. The effects of synthesis parameters such as pulsed current value, pulse time ( $t_{on}$ ), relaxation time ( $t_{off}$ ), temperature and concentrations of aniline, pyrrole and hydrochloric acid are studied and optimized by the “one factor at a time” method. The optimized conditions include 0.1 M pyrrole, 0.1 M aniline and 0.12 M hydrochloric acid, 9 mAcm<sup>-2</sup> current density, 1 s  $t_{on}$ , 1s  $t_{off}$  and solution temperature of 1°C. The synthesized nanomaterials are filtered and washed with 0.12 M hydrochloric acid solution and finally washed with double- distilled water. The obtained precipitate is dried at 80°C for 90 min under vacuum. The synthesized samples are characterized by SEM, TEM, DLS, TGA/DTA, IR spectroscopy, UV- Vis spectroscopy and Cyclic Voltammetry. The final sample consisting spherical nanoparticles with mean diameter smaller than 10 nm.

---

**Keywords:** Polymer nanoparticles, aniline- pyrrole copolymer, electropolymerization, pulsed galvanostatic method

### 1. INTRODUCTION

As an outcome of the developments in polymer technology, conductive polymers can act as substitutes for naturally conductive materials [1]. In last decade, great concerns have been focused to the conductive polymers such as polyaniline (PAni), polypyrrole (PPyr), polythiophen, polyparaphenylene, polyacetylene, and etc [2]. Conductive polymers are being commonly used in

various applications such as rechargeable batteries [3,4], production of semiconductor photoanodes [5], electrochemical displays [6], data storage devices [7], and biochemical analysis [8].

As a wide application area has inevitably encouraged research in the field of electro-conducting polymers, mainly directed towards obtaining improved properties. The synthesis of copolymers (containing two or more monomers) is the accepted method to change the properties of the polymers and obtain the desired specifications. There are many reports about the synthesis of various copolymers. In all of them, achieving of the desired properties is the main objective. One major problem that limits the availability of conductive polymers is the rareness of the conjugated  $\pi$ -bond containing monomers that are essential for their synthesis. The copolymerization as well as provides better properties, help to overcome this limitation as the number of conductive polymers obtained from the same monomer is increased. Consequently, it becomes possible to pick out superior properties of the individual monomers that polymerizing different environments and combine them together.

Polyaniline (PAni) and Polypyrrole (PPyr) are the famous conductive polymers with appropriate properties such as high electrical conductivities and good stability in the air. Both PAni and PPyr have better performance as cathode of rechargeable batteries [9-13]. The reasonable expectation is that the aniline/pyrrole copolymerization can improve their properties, especially in rechargeable batteries. Copolymerization of aniline and pyrrole can be done through chemical [14-17] and electrochemical methods [1]. The electropolymerization has many advantages including simplicity in preparation and controlling the termination step of polymerization. The electrochemically synthesized conductive polymers are purer than those of chemical polymerization due to the absence of additional chemical species such as surfactants, oxidants, and so on.

The reported electrosynthesis methods for the preparation of conductive polymers include potentiostatic [18-25], galvanostatic [26,27], cyclic voltammetry [28-33], pulse potentiostatic [34-39], pulse galvanostatic [40-43], and step-wise galvanostatic [44,45] methods. In the pulse galvanostatic electrosynthesis method, the controlling of particle size and the morphology of the samples are easy. The pulse current method can be used in double electrode cells so, it can be used in laboratory and industrial scales [2].

In this work, aniline/pyrrole (APC) nanoparticles are synthesized by applying the pulse current into a double- electrode cell containing aniline, pyrrole and HCl. The effective parameters of the morphology and size of the APC nanoparticles including the pulse amplitude, pulse time, relaxation time, aniline concentration, pyrrole concentration, acid concentration and solution temperature which are investigated and optimized by the "one factor at a time" method.

## 2. EXPERIMENTAL

### 2.1. Materials

Aniline, pyrrole, hydrochloric acid and dimethyl sulfoxide (DMSO) were purchased from Merk. Next, Aniline and pyrrole were distilled and stored in the dark sealed vessels. In all experiments, double- distilled water was used.

## 2.2. Instrumental

All the electrosynthesis experiments were carried out by an pulsed electrolyzer (BTE 04, made in Karami technical group, Iran). Cyclic Voltammetry (CV) experiments were performed by Autolab (Eco Chimie, PGSTAT-10, Netherland). The pores of porous graphite electrodes were mechanically filled with the synthesized APC nanoparticles and was used as the working electrode in all CV experiments. An Ag/AgCl reference electrode and a platinum counter electrode were used in electrochemical studies. FT- IR spectrophotometer (JASCO1600, Japan) was used to identify the chemical functional groups of APC nanoparticles. The morphology and particle size of the samples were characterized by scanning electron microscopy (SEM, Cam Scan, MV 2300, England) and transmission electron microscopy (TEM; ZEISS EM900). Uv-Visible spectra were measured using a double- beam spectrophotometer (GBC 197, Australia). Thermogravimetric analysis (TGA) was performed using a thermogravimetric analyzer (Perkin Elmer Thermal analysis, USA) for thermal studies.

## 2.3. Synthesis procedure

Before each electrodeposition, one pair of cylindrical platinum grid electrodes was placed in the diluted  $\text{HNO}_3$  for 30 minutes and then rinsed with double- distillate water to clean any surface pollutant. The grid electrodes were coupled together to coaxial form and put them in the electrochemical cell. The smaller Pt grid electrode was connected to the positive pole of the electrolyzer to act as the anode. The electrosynthesis cell was filled with a mixed solution containing 0.1 M aniline, 0.1 M pyrrole and 0.12 M hydrochloric acid at a temperature of  $1^\circ\text{C}$ . The Nitrogen gas was purged through the solution to remove dissolved oxygen. The current density of  $9 \text{ mAcm}^{-2}$ ,  $1 \text{ s } t_{\text{on}}$ ,  $1 \text{ s } t_{\text{off}}$  and the temperature of  $1^\circ\text{C}$  was inserted into the cell for 3 h while the solution was stirred. The synthesized APC nanoparticles was filtered and washed first using 0.12 M hydrochloric acid and finally double-distilled water. The collected paste was then vacuum-dried at  $80^\circ\text{C}$  for 90 min. The effects of some effective parameters such as pulse time ( $t_{\text{on}}$ ), relaxation time ( $t_{\text{off}}$ ) and temperature were varied and optimized by the “one factor at a time” method. Finally, all the synthesized samples were studied by SEM. Four samples were selected to more characterize by Uv-Vis spectroscopy, cyclic voltammetry and measurement of electrical conductivity. Optimized sample was characterized by IR spectroscopy, TGA, TEM and DLS.

## 3. RESULTS AND DISCUSSION

In the current study, APC synthesis was done by using the pulsed current method on the Pt grid electrode from a solution including aniline, pyrrole and HCl. Figure 1 shows a DC current pulse diagram that was used. Based on Fig. 1, the current pulse has three variables including pulse height, pulse time ( $t_{\text{on}}$ ) and relaxation time ( $t_{\text{off}}$ ).

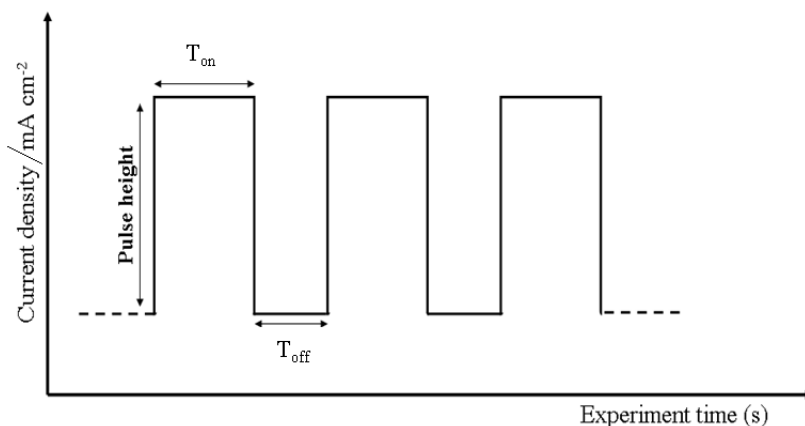
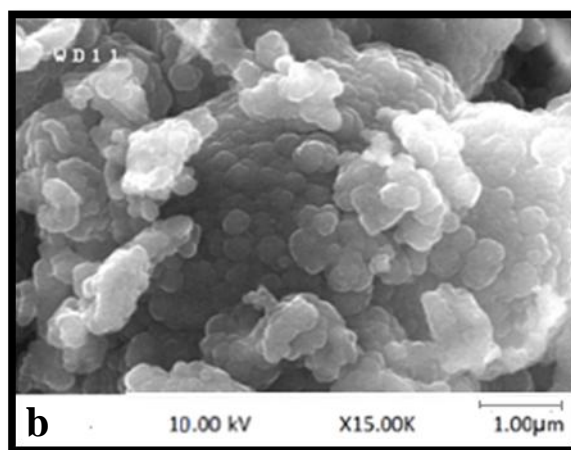
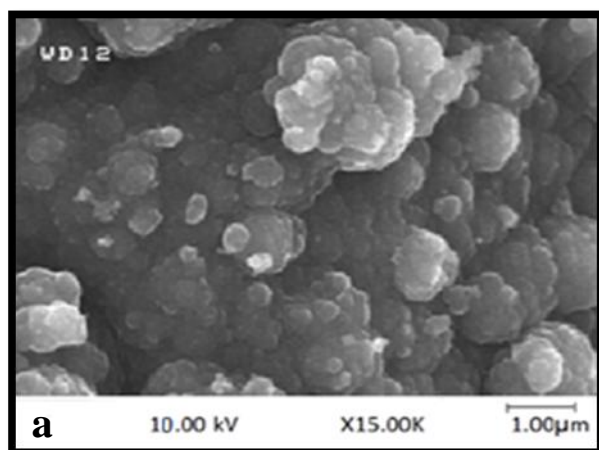


**Figure 1.** The used pulsed current diagram.

Addition to the mentioned parameters in Fig. 1, the present method consisting chemical parameters such as synthesis temperature and aniline, pyrrole and acid concentrations. In this work, the optimized values of some parameters such as pulsed current density ( $9\text{mAcm}^{-2}$ ), pyrrole concentration (0.1 M), aniline concentration (0.1 M) and hydrochloric acid concentration (0.12 M) from previous reports were taken and were constant in all experiments of this work [2,46]. The other parameters were fully studied.

### 3.1. Optimization of pulse time ( $t_{on}$ )

The effects of pulse time on the morphology and particle size of APC samples were investigated. To study the effects of pulse time, five samples were synthesized at different pulse times (0.25 s, 0.5 s, 1 s, 1.5 s and 2 s). In these experiments, the pulse current density,  $t_{off}$ , temperature, aniline, pyrrole and HCl concentrations were  $9\text{mAcm}^{-2}$ , 1 s,  $30^\circ\text{C}$ , 0.1 M, 0.1 M and 0.12 M, respectively. Figure 2 shows the SEM images of the APC samples.



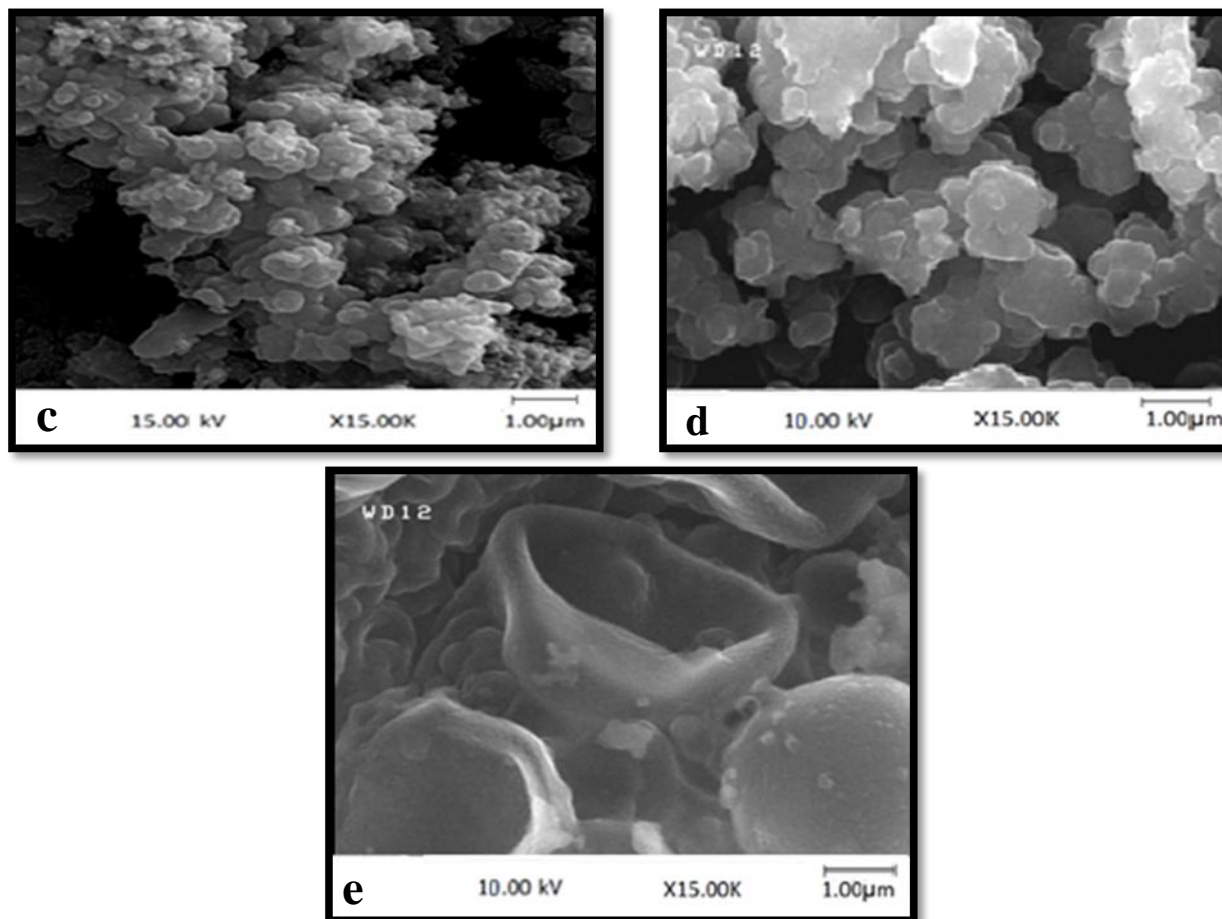


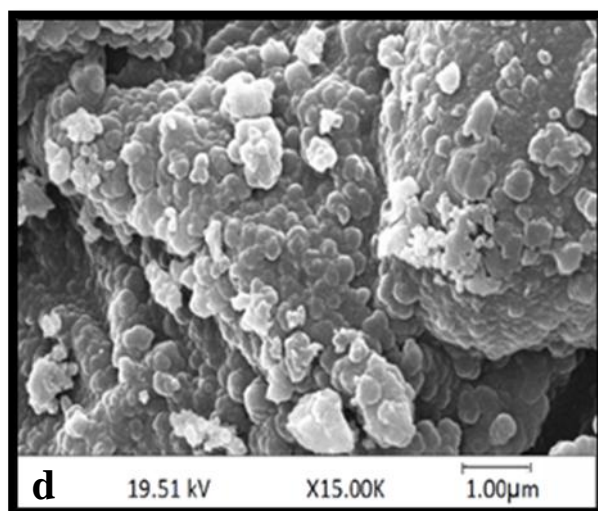
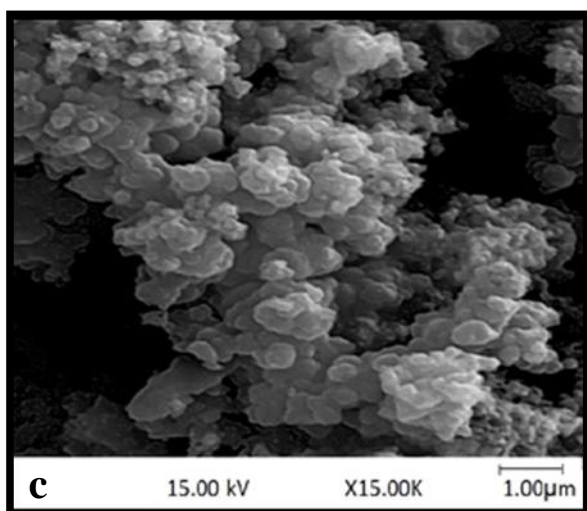
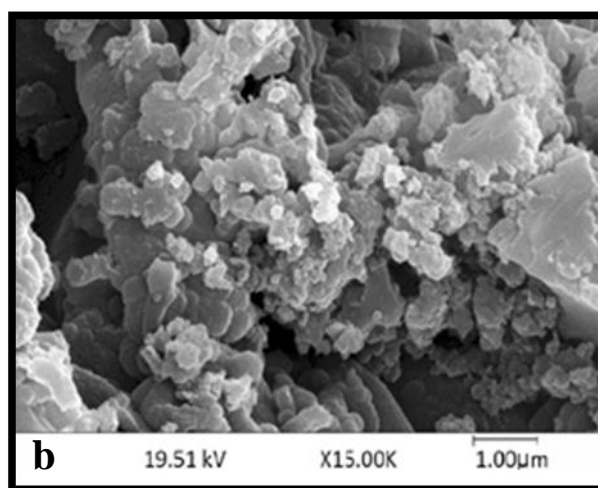
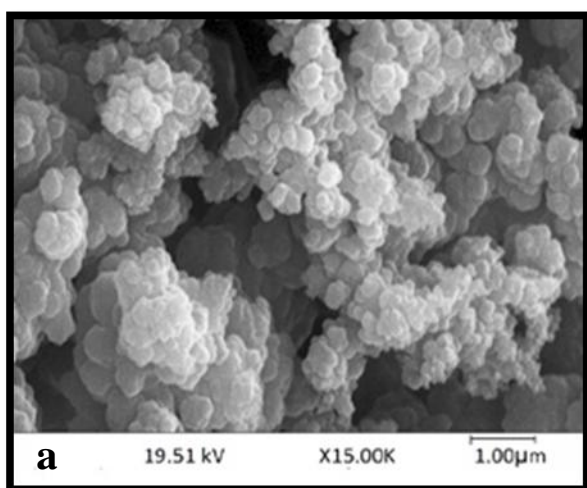
**Figure 2.** SEM images of the APC samples synthesized in  $9\text{mAcm}^{-2}$  pulsed current,  $30^\circ\text{C}$  temperature,  $0.1\text{ M}$  pyrrole,  $0.1\text{ M}$  aniline and  $0.12\text{ M}$  hydrochloric acid and with different pulse times  $0.25\text{ s}$  (a),  $0.5\text{ s}$  (b),  $1\text{ s}$  (c),  $1.5\text{ s}$  (d) and  $2\text{ s}$  (e).

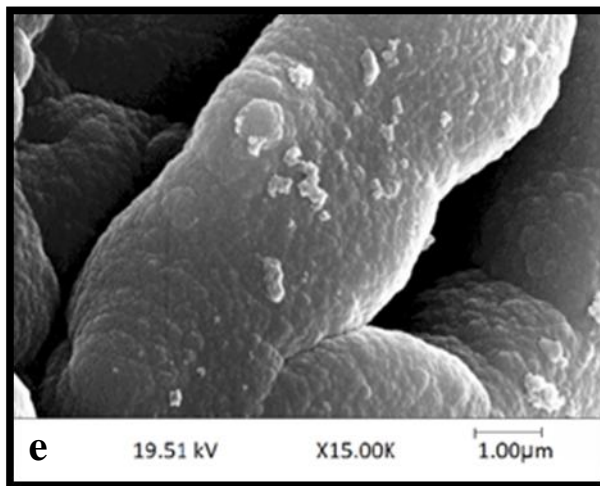
As it can be seen in Fig. 2, the pulse time can strongly change the morphology and particle size of the samples. Based on the presented SEM images, pulse time of  $1\text{ s}$  cause to form more uniform nanoparticles with a smaller diameter than the others (Fig. 2c). There are a calculable number of electrons in each current pulse that varies as well as pulse time [2]. During the application of the pulse, aniline- pyrrole copolymer nanoparticles are formed. The morphology and particle size of the APC samples are changed as well as the number of electrons. At the beginning of each current pulse, the nucleation rate is faster than that's of particle growth [47] but, at the end of each current pulse, the situation is reversed [2]. Therefore, the pulse time as an important parameter can affect on the morphology of and the particle size of the samples.

When a current pulse is turned on, there is a big charge transfer impedance, which causes the cell potential to increase and overcome the impedance barrier. In each pulse, a major part of the pulse time is spent on increasing the potential [2]. Once the cell potential has reached the suitable value, the oxidation of aniline and pyrrole will start. Based on the presented data, the best value of the pulse time is  $1\text{ s}$ .

### 3.2. Optimization of relaxation time ( $t_{off}$ )

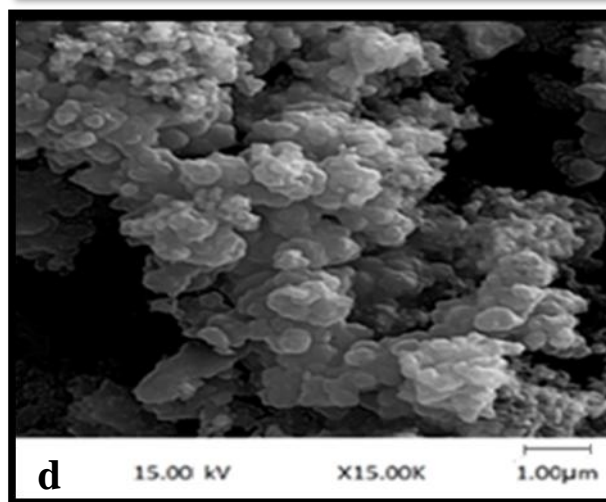
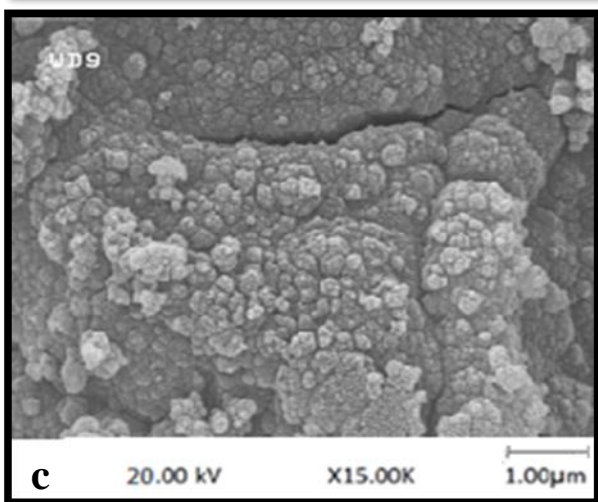
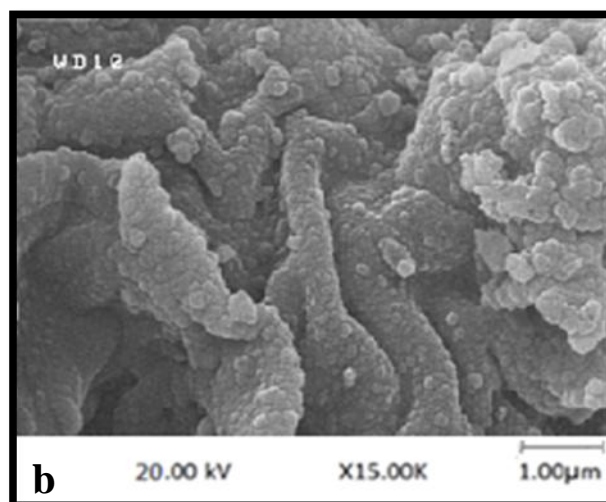
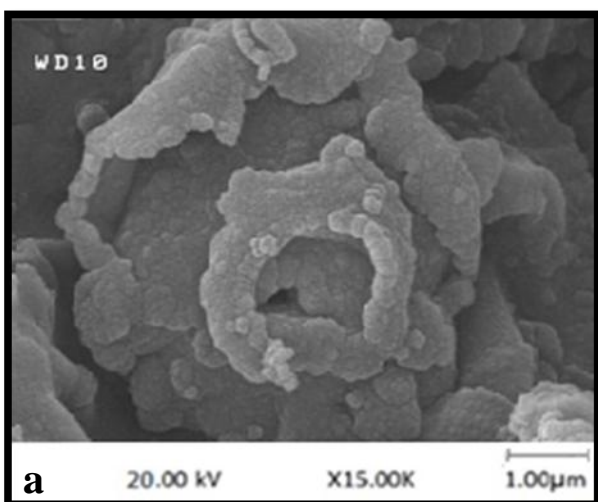
In order to investigate the effects of relaxation time on the morphology and particle size of the synthesized APC, we apply different relaxation times (0, 0.25 s, 0.5 s, 1 s, 2 s and 3 s). In these experiments, the pulse current amplitude,  $t_{on}$ , temperature, aniline, pyrrole and HCl concentrations were  $9 \text{ mA cm}^{-2}$ , 1 s,  $30^\circ\text{C}$ , 0.1 M, 0.1 M and 0.12 M respectively. The SEM images of APC samples which were synthesized at different relaxation times were shown in Fig. 3. The SEM images indicate that when the  $t_{off}$  is 1 s, it leads to more uniform nanoparticles and smaller diameters than the others. Pulse on time is a main factor that controls polymer chain size and chain defects [48]. The relaxation time in pulse electropolymerization is the another important factor can change the mechanism of the particle growth [2]. At low relaxation times, aniline-pyrrole copolymer nanoparticles are more agglomerated and the particles are not completely isolated because the relaxation time between two consequent current pulses is so short that before the particle formation is completed in the first pulse, the next pulse is applied, the next particle begins to be formed and connected to the last particle. At the longer relaxation time, the synthesized nanoparticles have rearrangement to further. Thus, using the longer relaxation time than 1 s cause the non-desirable morphology of synthesized samples. Therefore, relaxation time of 1s can be used as the best value for the synthesis of APC nanoparticles.





**Figure 3.** SEM images of the APC samples synthesized in  $9 \text{ mAcm}^{-2}$  pulsed current,  $1 \text{ s } t_{\text{on}}$ ,  $30^\circ\text{C}$  temperature,  $0.1 \text{ M}$  pyrrole,  $0.1 \text{ M}$  aniline and  $0.12 \text{ M}$  hydrochloric acid and with different relaxation times:  $0 \text{ s}$  (a),  $0.25 \text{ s}$  (b),  $0.5 \text{ s}$  (c),  $1 \text{ s}$  (d),  $2 \text{ s}$  (e) and  $3 \text{ s}$  (f).

### 3.3. Optimization of synthesis temperature



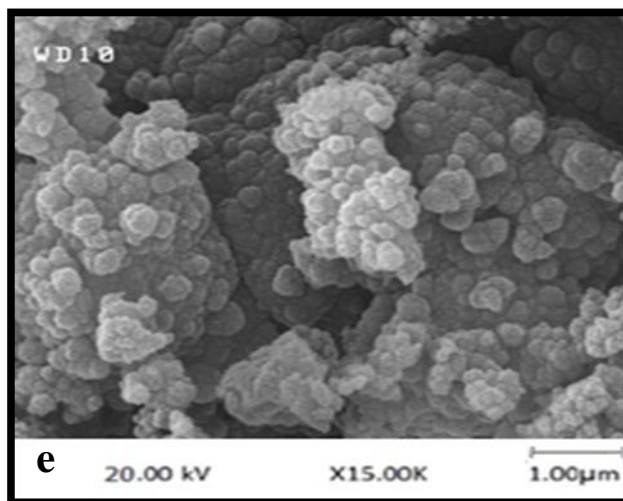


**Figure 4.** SEM images of the APC samples synthesized in  $9 \text{ mAcm}^{-2}$  pulsed current,  $t_{\text{on}} 1 \text{ s}$ ,  $t_{\text{off}} 1 \text{ s}$ ,  $0.1 \text{ M}$  pyrrole,  $0.1 \text{ M}$  aniline and  $0.12 \text{ M}$  hydrochloric acid and with different temperatures:  $1 \text{ }^{\circ}\text{C}$  (a),  $10 \text{ }^{\circ}\text{C}$  (b),  $20 \text{ }^{\circ}\text{C}$  (c),  $30 \text{ }^{\circ}\text{C}$  (d) and  $40 \text{ }^{\circ}\text{C}$  (e).

As explained in our previous studies [2,46,49-54], the synthesis temperature is an effective parameter in the controlling of morphology and particle size of the electrosynthesized particles. Five samples were synthesized at different temperatures ( $1 \text{ }^{\circ}\text{C}$ ,  $10 \text{ }^{\circ}\text{C}$ ,  $20 \text{ }^{\circ}\text{C}$ ,  $30 \text{ }^{\circ}\text{C}$  and  $40 \text{ }^{\circ}\text{C}$ ). In these experiments, the pulse value,  $t_{\text{on}}$ ,  $t_{\text{off}}$ , aniline, pyrrole and HCl concentrations were  $9 \text{ mAcm}^{-2}$ ,  $1 \text{ s}$ ,  $1 \text{ s}$ ,  $0.1 \text{ M}$ ,  $0.1 \text{ M}$  and  $0.12 \text{ M}$ , respectively. Figure 4 shows the SEM images of APC samples which were synthesized at different temperatures.

The SEM images indicate the synthesis temperature can change the morphology and particle size of APC. Based on the previous report, electropolymerization temperature has a substantial influence on the mechanical characterization as well as on conductivity and redox properties of the final sample [55]. It should be noted that a decrease in the redox properties is observed as the temperature increases. At higher temperatures, interfering reactions such as solvent treatment and nucleophilic attacks on polymeric radicals make some structural defects in polymer, resulting in low conductive APC. Usually, higher conductivities of polymers can be achieved at lower temperatures [56,57] and the overall reactions are favored by lower reaction temperatures in acidic media [58]. Based on Fig. 4, the sample synthesized at  $1 \text{ }^{\circ}\text{C}$  has the smallest and most uniform nanoparticles. Therefore, to obtain an APC sample with the highest conductivity and smallest particles, synthesis can be done at the lowest temperature ( $1 \text{ }^{\circ}\text{C}$ ). In this temperature, the produced sample was black in color.

#### 3.4. Characterization of synthesized aniline-pyrrole copolymer nanoparticles

Based on the optimization set (sections 3-1 to 3-3), the optimized conditions for the synthesis of APC nanoparticles by the pulse electropolymerization method are  $9 \text{ mAcm}^{-2}$  current density,  $1 \text{ s}$  relaxation time,  $1 \text{ s}$  pulse time,  $1 \text{ }^{\circ}\text{C}$  solution temperature,  $0.1 \text{ M}$ ,  $0.1 \text{ M}$  pyrrole and  $0.12 \text{ M}$  hydrochloric acid. The SEM images of the optimized APC nanoparticles in four magnifications were shown in Fig. 5.

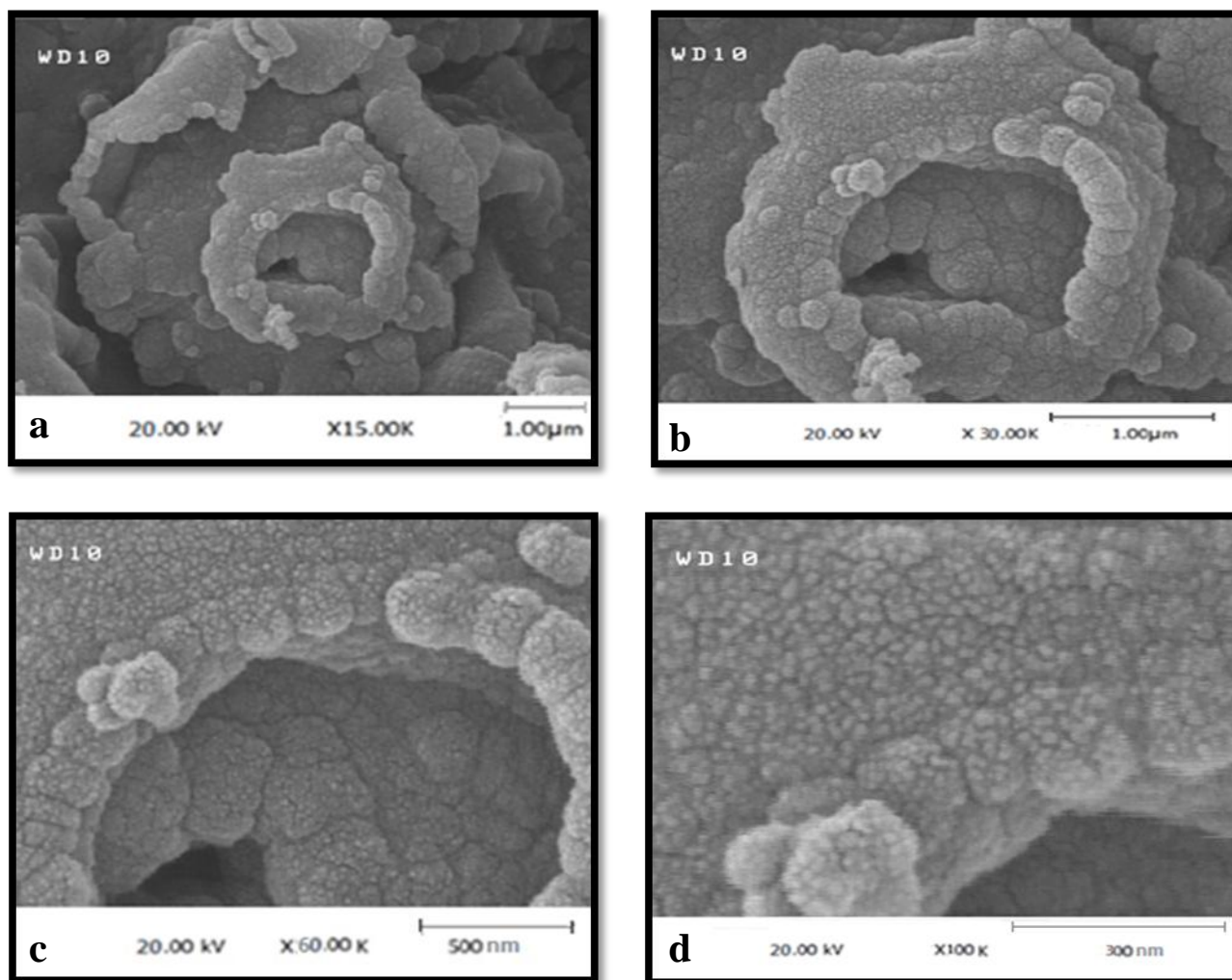


**Figure 5.** SEM images of the optimized APC nanoparticles in four magnifications: 15000 (a), 30000 (b), 60000 (c) and 100000 (d).

Based on these SEM images, the sample contains nanoparticles with 20 nm mean diameter. For more clarifications, the optimum sample was analyzed by TEM and DLS. Figure 6 shows the DLS diagram and TEM micrograph. TEM and DLS results show that the sample containing nanoparticles with average diameter lower than 10 nm.

Figure 7 displays the FT-IR spectrum of the optimized APC nanoparticles. FT-IR spectroscopy was used to characterize the molecular structure of the optimized APC nanoparticles.

According to Fig. 7, 500 to 900 $\text{cm}^{-1}$  absorption bands attributed to the bending vibrations of C-H bonds and 1350 to 1000  $\text{cm}^{-1}$  absorption bands attributed to C-N bonds [59]. Vibration bands of pyrrole ring are located at 1547 and 1461 $\text{cm}^{-1}$  [60]. According to another study [60], absorption band at 3425  $\text{cm}^{-1}$  attributed to aromatic N-H bonds stretching vibrations in PPy, but in this study, position of this absorption bond has low change and is 3432.67  $\text{cm}^{-1}$ . Also, in other study [61], the absorption band of C=C bonds stretching, vibrations benzenoid rings in PANi reported at 1490  $\text{cm}^{-1}$ , but in this study, position of this absorption bond has low change and it is 1427.07  $\text{cm}^{-1}$ . Therefore, this changes

in position of this absorption bands can related to the bonding between aniline and pyrrole in synthesized APC.

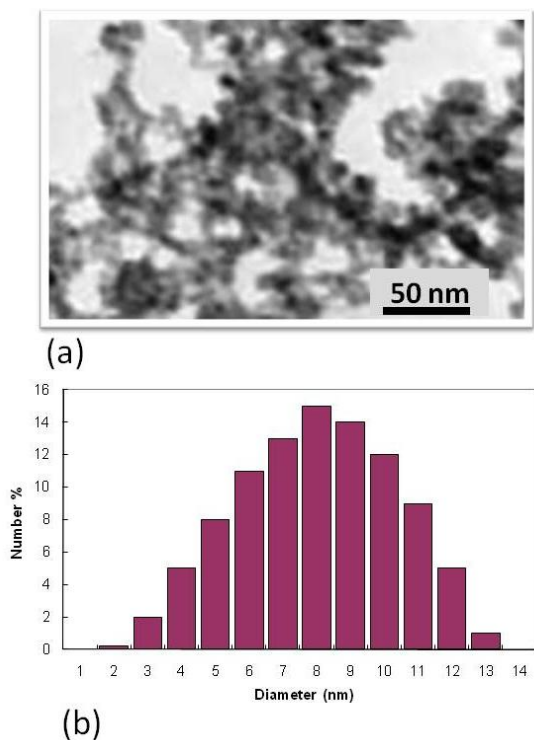


**Figure 6.** TEM image and DLS diagram for APC nanoparticles

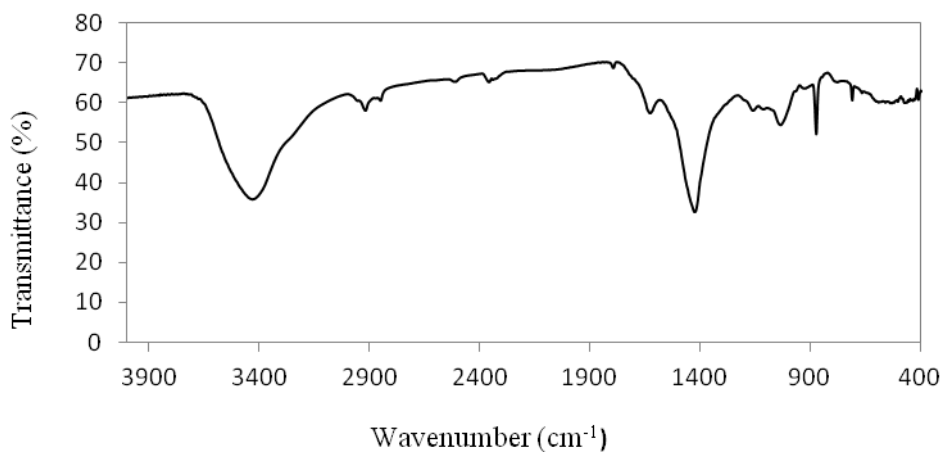


**Figure 7.** FT-IR spectrum of the APC nanoparticles synthesized in the optimum conditions

### 3.5. Electrochemical studies

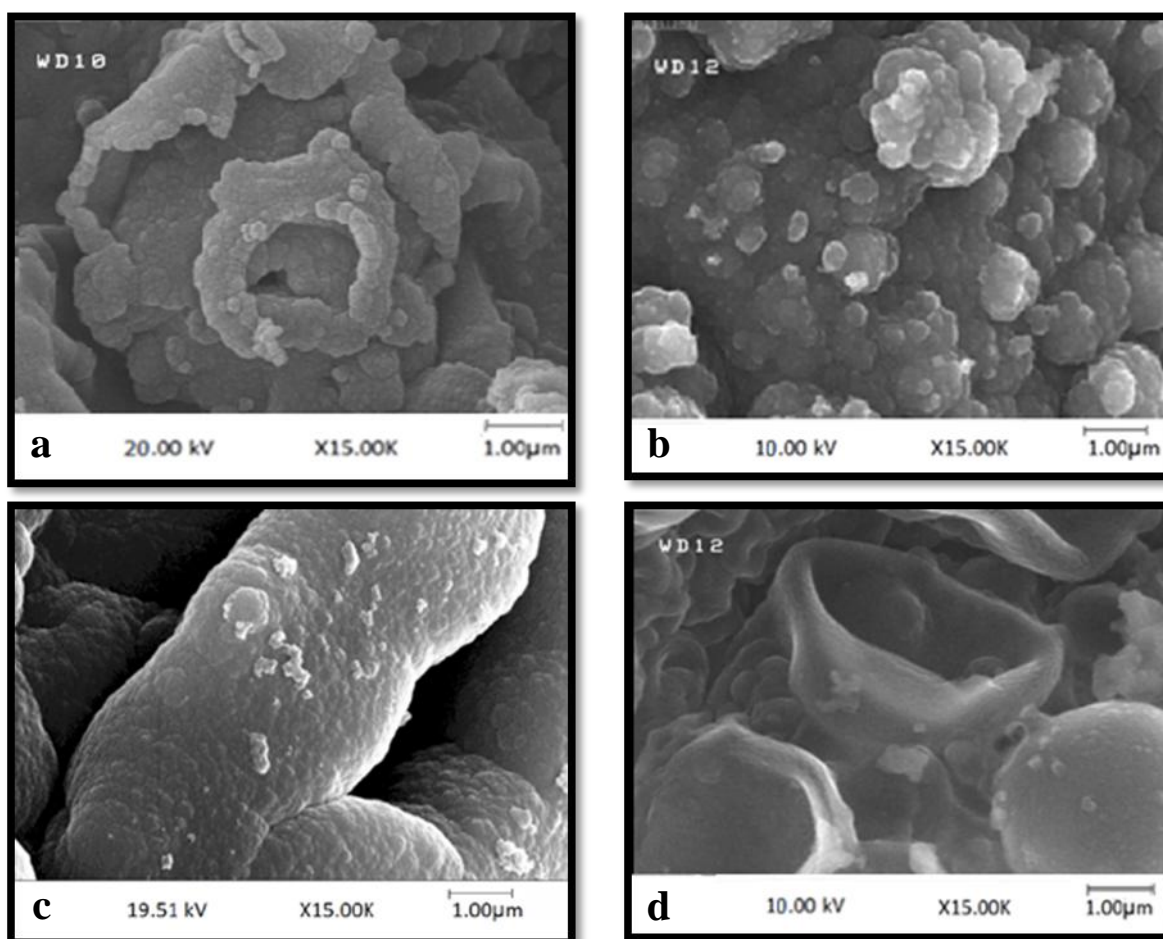
To investigate the effect of morphology on the electrochemical behavior of APC, four experimental conditions from the experimental set (section 3.1 to 3.3) were chosen (Table 1) and four APC samples were synthesized in the selected conditions.

**Table 1.** Four different synthesis conditions selected for synthesizing of different APC samples for electrochemical studies.

Sample	Puls current (mAcm <sup>-2</sup> )	t <sub>on</sub> (s)	t <sub>off</sub> (s)	Aniline (mol dm <sup>-3</sup> )	Pyrrol (mol dm <sup>-3</sup> )	HCl (Mol dm <sup>-3</sup> )	Temperature (°C)
a	9	1.00	1	0.1	0.1	0.12	1
b	9	0.25	1	0.1	0.1	0.12	30
c	9	1.00	3	0.1	0.1	0.12	30
d	9	2.00	1	0.1	0.1	0.12	30

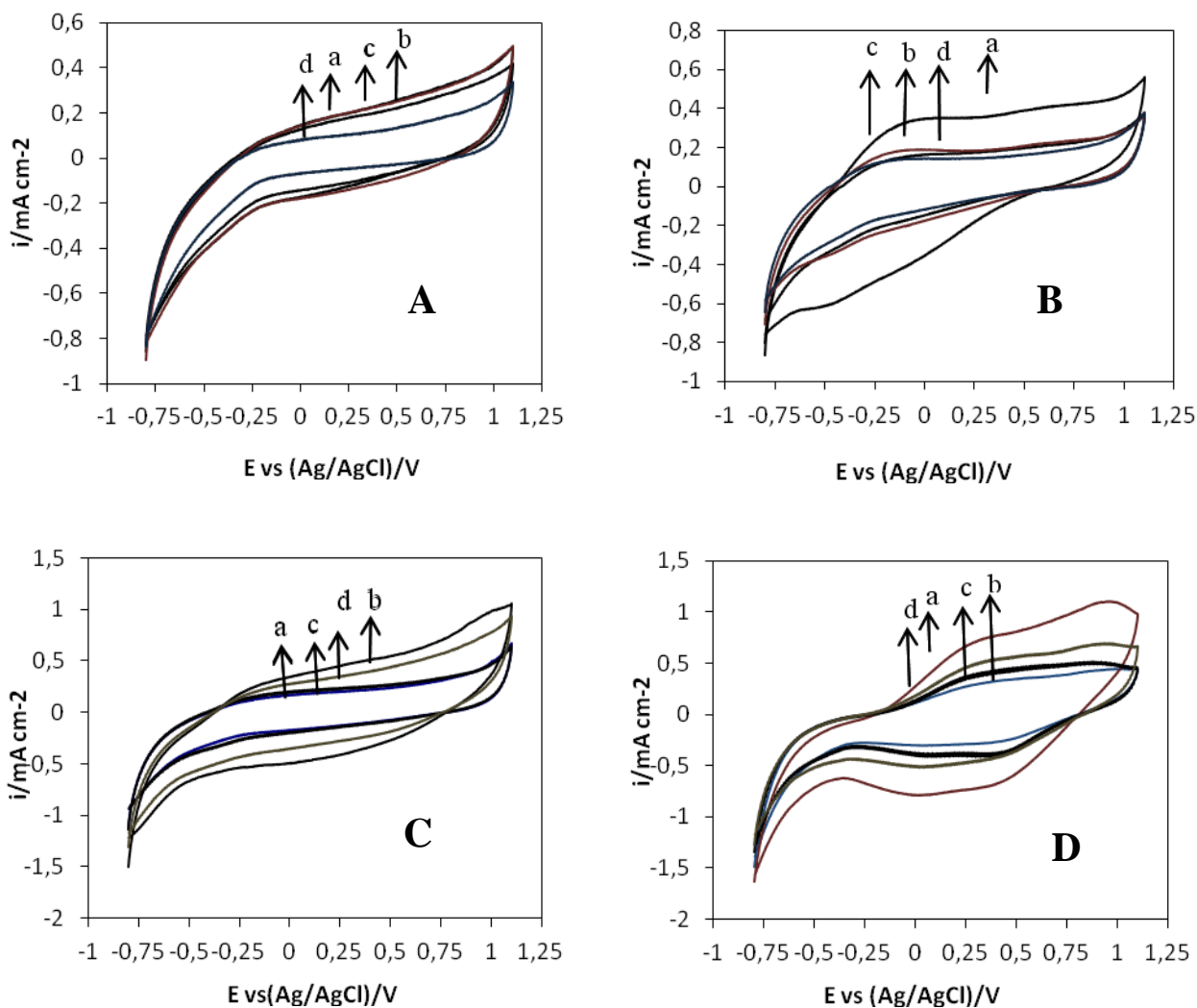
\* (optimized sample)

Figure 8 shows the SEM images of the selected samples that synthesized according to the Table1. As it can be seen in Fig. 8. The APC sample have different morphologies and particles sizes.

**Figure 8.** SEM images of four APC samples which synthesized under the different conditions according to Table 1. The a, b, c and d samples were introduced in Table 1.

Many factors, including the electrolyte type, potential scan rate and aniline- pyrrol copolymer morphology can change the voltammograms of APC nanoparticles.

To investigate the effect of electrolyte on the CVs, four electrolytes including 0.1 M barium perchlorate, 0.2 M sodium benzoate, 1 M potassium chloride and 0.12 M hydrochloric acid, were used for obtaining of CVs of the APC samples1 with 100 mV/s potential scan rate in the potential range of -0.8 V to 1.1 V versus Ag/AgCl reference electrode. Figure 9 displays CVs of the synthesized samples of Table 1 in the different electrolytes.



**Figure 9.** The effects of electrolyte type on the CVs of the synthesized APC samples: (A) barium perchlorate 0.1 M, (B) sodium benzoate 0.2 M, (C) potassium chloride 1 M (D) hydrochloric acid 0.12 M. In all curves, a, b, c and d are the samples labels according to Table 1. All CVs were taken with 100 mV/s potential scan rate.

According to Fig. 9, the 0.12 M hydrochloric acid is suitable electrolyte for this cyclic voltammetry studies, because the cyclic voltammetry diagrams of this electrolyte have more obvious

peaks than other diagrams. The observed result is related to this fact that the doping and dedoping of polymer depends strongly on hydrogen and chloride ions. The hydrochloric acid solution can provide enough both hydrogen and chloride ions. Therefore, redox reactions can be fastly carried out. As it can be seen in Fig. 9, in all cyclic voltammograms (CVs), two pairs of redox peaks are observed. The first pair of redox peaks occurs in the potential range of -0.3 V to 0.4 V (vs. Ag/AgCl reference electrode) indicates the reversible transformation of Leucoemeraldine into Emeraldine salt in PANi department of aniline-pyrrole copolymer. During conversion of Leucoemeraldine to Emeraldine salt, both oxidation and doping of chloride ions are done. The second pair of redox peaks occurs in the potential range of 0.4 V to 1 V which is attributed to the transformation of emeraldine salt into pernigraniline in PANi [2]. These peaks are characteristic of PANi's conversions between the different doping states [62]. The width of the peaks suggests that these doping and undoping processes are complex [63]. Therefore, According to the CVs shown in Fig. 9, the optimized APC (sample a) has a higher redox kinetics (based the peak current). The obtained result is related to the smaller particles of sample a than those of other samples. The improved performance of polymer is attributed to the presence of a lesser density of defects in polymer structure during polymerization by pulsed technique.

For more study, the effect of potential scan rate was investigated on the CVs of the sample a (The optimized sample in Table 1). Eventually, scan rates of 20, 40, 60, 80, 100, 120, 140 and 160 mV/s were used for cyclic voltammetry of the optimized sample in 0.12 M hydrochloric acid electrolyte and -0.8 V to 1.1 V potential range of scan respectively (Fig. 10).

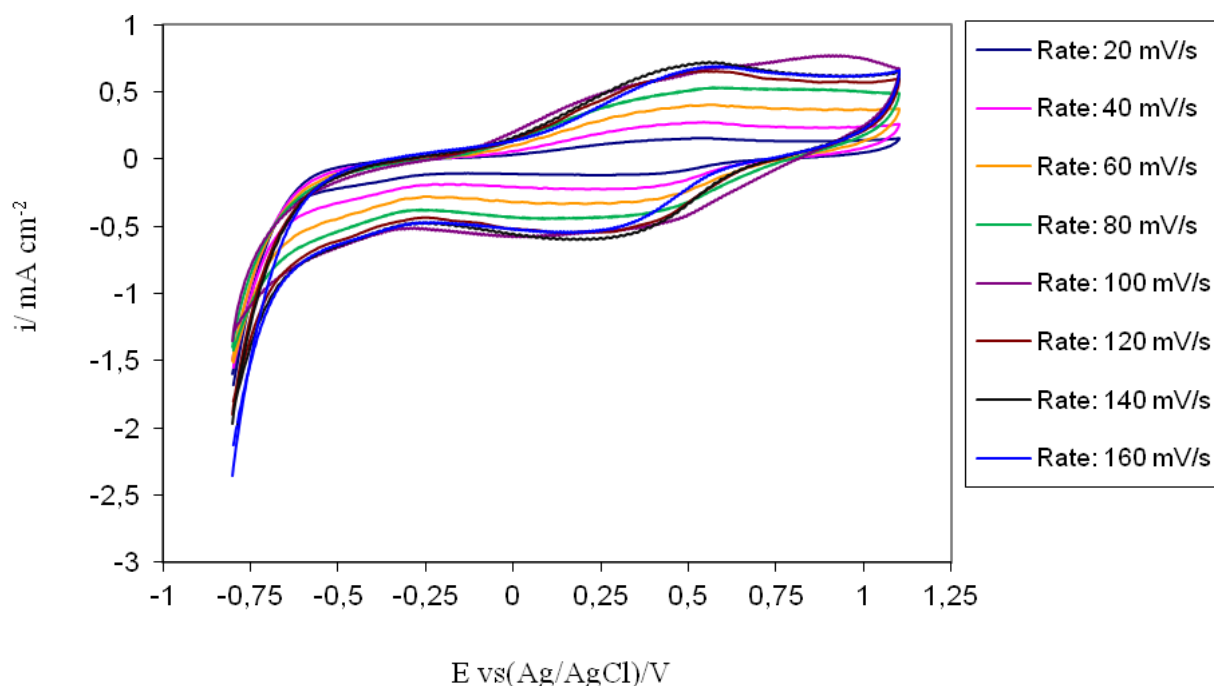


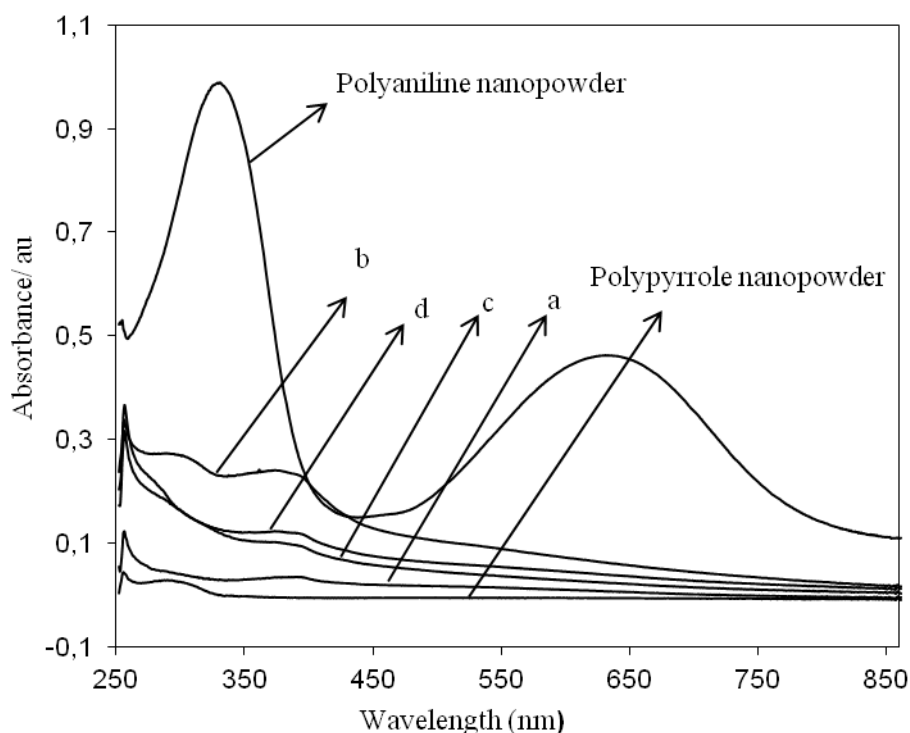
**Figure 10.** CVs of the optimized sample (sample a in Table 1) in different scan rates in 0.12 M HCl electrolyte.

According to Fig. 10, the 140 mV/s is suitable scan rate for the cyclic voltammetry studies, because the cyclic voltammetry diagrams of this scan rate have more obvious peaks than other diagrams.

### 3.6. Additional studies

#### 3.6.1. Uv-Vis spectroscopic studies

UV-Vis spectroscopy is a powerful technique to show any change in the molecular structure and chromophore groups. Figure 11 shows the spectrums of the samples a, b, c and d as well as PANi and PPy.



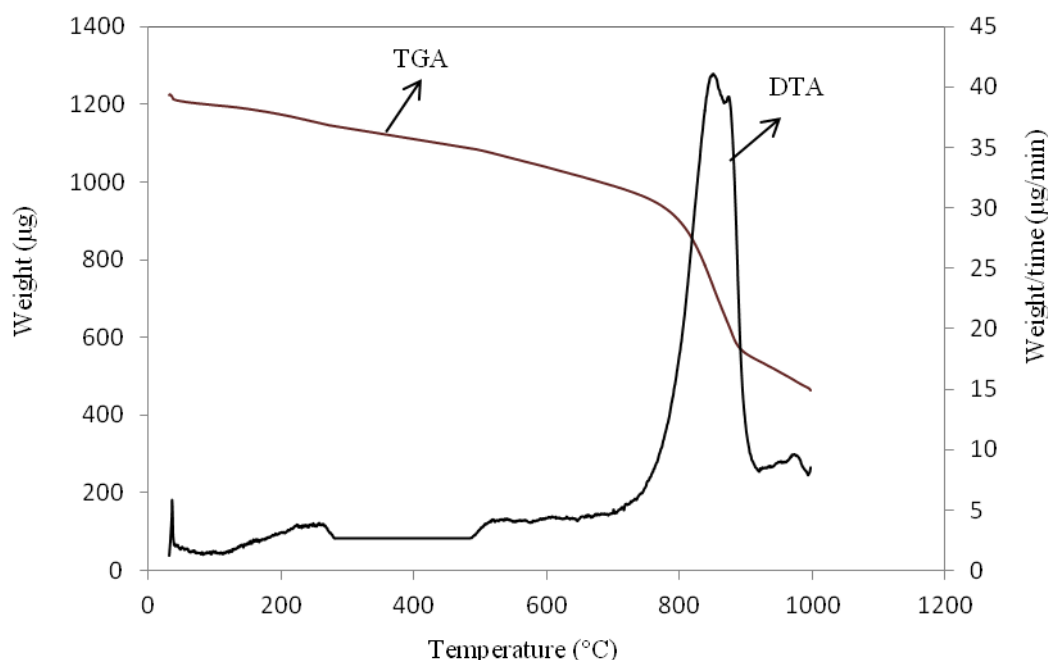
**Figure 11.** Uv-Vis spectrums for PANi nanopowder, PPy nanopowder and APC samples a, b, c and d according to Table 1. All samples were dissolved in DMSO to obtain saturated solution for Uv-Vis spectrometric studies.

Figure 11 shows the Uv-Vis spectrums of four APC samples synthesized under different conditions, according to Table 1, PPy nanopowder [46] and PANi nanopowder [2]. Samples a, b, c and d have the same spectrums but with different absorbances because these samples have different solubilities in MSO. According to a, b, c and d samples spectrums, the peak at 260 nm represent the  $\pi \rightarrow \pi^*$  transition of the pyrrole rings in APC. The peak at 300 nm can attributed to the  $\pi \rightarrow \pi^*$  transition of the benzenoid segment of PANi in APC. The peak at 390 nm can related to the protonated emeraldine form of PANi or polaron form of PPy in APC. There are blue shifts for the peaks of aniline and pyrrole in all APC samples in the presented Uv-Vis spectrums in comparison with those of pure

PAni and PPy nanpowders. The seen blue shifts is due to the bonding between aniline and pyrrole rings in APC formation.

### 3.6.2. Thermal analysis

Thermal gravimetric analysis (TGA) and Differential thermal analysis (DTA) were used for additional studies of the optimized APC (sample a in Table 1). Figure 12 shows the Taniline-pyrrole copolymer sample which was prepared under optimum conditions.



**Figure 12.** TGA/DTA thermographs of the optimized APC sample

Figure 12 shows that the APC is relatively stable in the thermal range of 25 to 850 °C. TGA diagram for the synthesized sample under optimum conditions. The copolymer is decomposed at 850 °C. The seen decomposition temperature is high than those of the previous reports [1, 17]. The decomposition temperature of pure PAni and pure PPy were reported 225 [2] and 273°C [1], respectively. The higher decomposition temperature shows the APC has more thermal stability than those of the previous reports. Figure 12 shows a gradually decreasing in the weight of APC sample 25 to 800 °C. In conductive polymers, this gradual weight loss is related to undoping of polymers.

### 3.6.3. Electrical conductivity

The electrical conductivity is one of the main factors of charge/discharge ability of PAni and PPy as positive materials of the rechargeable batteries. The electrical conductivities of the synthesized samples were measured by the direct two probes method. The results of electrical conductivities of the synthesized samples (according to Table 1) together with those of pure PAni [15] and pure PPy [46] were summarized in Table 2.

**Table 2.** The results of electrical conductivity measurements in the APC samples (samples a, b, c and d according to Table 1) in comparing with the reported conductivities for PANi [41] and PPyr [10].

Sample	a	b	c	d	PPyr	PAni
Conductivity (mScm <sup>-1</sup> )	37	40	84	665	20	470

As it can be seen in Table 2, the electrical conductivity of the sample d, is higher than other samples. According to Fig. 8, the hollow spheres particles were formed in sample d. These hollow spheres connected together. Thus, particles in sample d have a good connection with together and have more electrical conductivity than other samples. As it can be seen in Table 2, APC samples (a, b, c and d) have more electrical conductivity than PPyr because the long conjugated  $\pi$ -bonds were formed with monomers of copolymers. Between four APC samples, sample a has a low conductivity. The sample a consisting uniform the smallest nanoparticles. The electrical contact between these nanoparticles are weaker than others.

#### 4. CONCLUSIONS

Nanostructured aniline/pyrrole copolymer (APC) can be prepared by the pulsed galvanostatic method. In this method, pulse time, relaxation time, synthesis temperature are the main parameters affecting on the morphology and the particle size of APC samples. The APC samples show the good reversibility in acidic solution in cyclic voltammetry technique so, they are suitable cathodic material in the rechargeable batteries. The APC sample show higher thermal stability than PANi and PPyr. The APC samples have higher electrical conductivities than PPyr and lower than pure PANi.

#### ACKNOWLEDGEMENT

The authors would like to thank the financial support of this work by Abhar Payame Noor University Research Council.

#### References

1. B. Sari, M. Talu, *Synth. Met.* 94 (1998) 221.
2. H. Karami, M. GhaleAsadi, M. Mansoori, *Electrochim. Acta*, 61 (2012) 154.
3. F. A. Taromi, H. Omidyan, *Polym. Sci. Technol.*, 2 (1989) 1.
4. T. Ojio, S. Miyata, *Polym. J.* 18 (1986) 95.
5. S. Dong, W. Zhang, *Synth. Met.* 30 (1989) 359.
6. C. K. Mann, *Electroanal. Chem.* 3 (1969) 57.
7. S. Kuwabata, S. Ito, H. Yoneyama, *J. Electrochem. Sci. Technol.*, 135 (1988) 1691.
8. D. T. Hao, T. N. Suresh Kumar, R. S. Srinisava, R. Lal, N. S. Punekar, A. Q. Contractor, *Anal. Chem.*, 64 (1992) 2645.

9. H. Karami, M.F. Mousavi, M. Shamsipur, *J. Power Sources*, 124 (2003) 303.
10. Karamil, A. Rahimi Nezhad, *Int. J. Electrochem. Sci.*, 8 (2013) 8905.
11. H. Karami, M. G. Asadi, M. Mansoori, *Electrochim. Acta*, 61 (2012) 154.
12. H. Karami, M. F. Mousavi, M. Shamsipur, S. Riahi, *J. power sources*, 154 (2006) 298.
13. H. Karami, M. F. Mousavi, M. Shamsipur, , *J. Power Sources*, 114 (2003) 303.
14. J. Stejskal, M. Trchová, I. A. Ananieva, J. Janča, J. Prokeš, S. Fedorova, I. Sapurina, *Synth. Met.*, 146 (2004) 29.
15. V. W. L. Lim, E. T. Kang, K. G. Neoh, Z. H. Ma, K. H. Tan, *Appl. Surf. Sci.*, 181 (2001) 317.
16. P. Xu, X. J. Han, C. Wang, B. Zhang, H. L. Wa, *Synth. Met.*, 159 (2009) 430.
17. Q. F. Lu, Z. W. He, J. Y. Zhang, Q. Lin, *Anal. Appl. Pyrol.*, 93 (2012) 147.
18. L. Hung, Zh. Wang, H. Wang, X. Cheng, A. Mitra, Y. Yan, *Mater. Chem.*, 12 (2002) 388.
19. Z. Tang, S. Liu, Z. Wang, S. Dong, E. Wang, *Electrochem. Commun.*, 2 (2000) 32.
20. A. Eftekhari, *Synth. Met.*, 145 (2004) 211.
21. M. Nakayama, J. Yano, K. Nakaoka, K. Ogura, *Synth. Met.*, 128 (2002) 57.
22. E. Munoz, A. Colina, A. Heras, V. Ruiz, S. Palmero, J. Lopez-Palacios, *Anal. Chim. Acta*, 20 (2006) 573.
23. S. Wang, Z. Line, L. Chen, J. Zhou, *Electrochim. Acta*, 55 (2010) 2727.
24. T. Wang, Y. J. Tan, *Corros. Sci.*, 48 (2006) 2274.
25. Y. C. Liu, K. H. Yang, *Electrochim. Acta*, 51 (2006) 5376.
26. K. Luo, N. Shi, C. Sun, *Polym. Degrad. Stab.* 91 (2006) 2660.
27. M. Bazzaoui, E. A. Bazzaoui, L. Martins, J. I. Martins, *Synth. Met.*, 128 (2002) 103.
28. D. Bejan, A. Duca, *Croat. Chem. Acta*, 71 (1998) 745.
29. M. C. Li, Ch. A. Ma, B.Y. Liu, Z. M. Jin, *Electrochem. Commun.*, 7 (2005) 209.
30. A. Baba, S. Tian, F. Stefani, C. Xia, Z. Wang, R. C. Advincula, D. Johann Smann, W. Knoll, *Electroanal. Chem.*, 562 (2004) 95.
31. X. Y. Zhao, J. B. Zang, Y. Zang, Y. H. Wang, L. Y. Bian, J. K. Yu, *Electrochem. Commun.*, 11 (2009) 1297.
32. C. Dalmolin, S. C. Canobre, S. R. Biaggio, R. C. Rocha-Filho, N. Bocchi, *Electroanal. Chem.*, 578 (2005) 9.
33. P. A. Mabrouk, *Synth. Met.*, 150 (2005) 101.
34. V. Tsakova, A. Milchev, *Electroanal. Chem.*, 346 (1993) 85.
35. H. Zhou, J. Wen, X. Ning, C. Fu, J. Chen, Y. Kuang, *Synth. Met.*, 157 (2007) 98.
36. H. F. Jiang, X. X. Liu, *Electrochim. Acta*, 55 (2010) 7175.
37. V. Rajendran, A. Gopalan, T. Vasudevan, W. C. Chen, T.C. Wen, *Mater. Chem. Phys.*, 65 (2000) 320.
38. H. H. Zhou, J. B. Wen, X. H. Ning, C. P. Fu, J. H. Chen, Y.F. Kuang, *Appl. Polym. Sci.*, 104 (2007) 458.
39. J. J. Langer, G. Framski, R. Joachimiak, *Synth. Met.*, 121 (2001) 1281.
40. S. Q. Jiao, H. H. Zhou, J. H. Chen, S. L. Luo, Y.F. Kuang, *Appl. Polym. Sci.*, 94 (2004) 1389.
41. H. H. Zhou, S. Q. Jiao, J. H. Chen, W. Z. Wei, Y.F. Kuang, *Thin Solid Films*, 450 (2004) 233.
42. H. Zhou, S. Q. Jiao, J. H. Chen, W. Z. Wei, Y. F. Kuang, *Appl. Electrochem.*, 34 (2004) 455.
43. G.A. Rambu, I. Stamatina, C. L. Jackson, K. Scott, *Optoelectron. Adv. Mater.* 8 (2006) 670.
44. L. Liang, J. Liu, C. F. Wndisch Jr, G. Exarhos, Y.H. Lin, *Angew. Chem. Int. Ed.*, 41 (2002) 3665.
45. H. Zhang, J. Wang, Z. Wang, F. Zhang, S. Wang, *Synth. Met.*, 159 (2009) 277.
46. H. Karami, A. Rahimi nezhad, *Int. J. Electrochem. Sci.*, 8 (2013) 8905.
47. S. Y. Cui, S. M. Park, *Synth. Met.*, 105 (1999) 91.
48. R. K. Sharma, A. C. Rastogi, S. B. Desu, *Electrochem. Commun.*, 10 (2008) 268.
49. H. Karami, M. Alipour, *Int. J. Electrochem. Sci.*, 4 (2009) 1511.
50. H. Karami, B. Kafi, S. N. Mortazavi, *Int. J. Electrochem. Sci.*, 4 (2009) 414.
51. H. Karami, A. Kaboli, *Int. J. Electrochem. Sci.*, 5 (2010) 706.

52. H. Karami, E. Mohammadzadeh, *Int. J. Electrochem. Sci.*, 5 (2010) 1032.
53. H. Karami, O. Rostami-Ostadkalayeh, *Clust. Sci.*, 20 (2009) 587.
54. H. Karami, S. Mohammadi, *Clust. Sci.*, 21 (2010) 739.
55. J. Rodrigues, H. J. Grande, T. F. Otero, "*Hand book of Organic Conductive Molecules and Polymers*", ed. H. S. Nalwa, John Wiley & Sons, New York, (1997).
56. M. Satoh, K. Kaneto, K. Yoshino, *Synth. Met.*, 14 (1986) 289.
57. M. Ogasawara, K. Funahashi, T. Demura, T. Hagiwara, K. Iwata, *Synth. Met.*, 14 (1986) 61.
58. S. U. Rahman, M. S. Ba-Shammakh, *Synth. Met.*, 140 (2004) 207.
59. D. L. Pavia, G. M. Lampmang, G. S. Kariz, "*Introduction to spectroscopy*", 2 nd, ed. Saunders (W. B) Co. Ltd., (1996).
60. L. Li, C. Xiang, X. Liang, B. Hao, *Synth. Met.*, 160 (2010) 28.
61. V. W. L. Lim, E. T. Kang, K. G. Neoh, Z. H. Ma, K. H. Tan, *Appl. Surf. Sci.*, 181 (2001)317.
62. S. Weng, Z. Lin, L. Chen, J. Zhou, *Electrochim. Acta*, 55 (2010) 2727.
63. N. C. T. Martins, T. Moura e Silva, M. F. Montemor, J. C. S. Fernandes, M. G. S. Ferreira, *Electrochim. Acta*, 53 (2008) 4754.

© 2016 The Authors. Published by ESG ([www.electrochemsci.org](http://www.electrochemsci.org)). This article is an open access article distributed under the terms and conditions of the Creative Commons Attribution license (<http://creativecommons.org/licenses/by/4.0/>).